ISSN (Print) 1226-1750
ISSN (Online) 2233-6656
Journal of Magnetics 23(4), 487-490 (2018) https://doi.org/10.4283/JMAG.2018.23.4.487

Weak Ferromagnetism and Exchange Bias in Antiferromagnetic Cobalt Oxide Nanoparticles

X. L. Wang[1], H. L. Ge[1]*, Q. L. Ye[2], P. Z. Si[1], and H. J. Chen[1]

[1]*College of Materials Science and Engineering, China Jiliang University, Hangzhou 310018, China*
[2]*Department of Physics, Hangzhou Normal University, Hangzhou 310036, China*

(Received 15 May 2018, Received in final form 19 September 2018, Accepted 11 October 2018)

The traditional arc discharge process for producing metallic nanoparticles was modified to be applicable for the direct preparation of oxide nanoparticles by using both conductive and insulative precursors. The cobalt oxide nanoparticles were synthesized by feeding Co and Co_2O_3 into the air plasma. The as-prepared nanoparticles are spherical in shape with size in the range of 10 to 40 nm. The phases of CoO and Co_3O_4 were detected in the samples prepared from the precursors of Co and Co_2O_3, respectively. Weak ferromagnetism and an exchange bias up to 17.1 mT were observed in these antiferromagnetic nanoparticles, owing to the presence of a large fraction of the uncompensated surface spins and possibly the local disordered regions.

Keywords : exchange bias, nanoparticles, cobalt oxide, arc discharge

1. Introduction

The cobalt oxide nanoparticles are widely used in fields such as catalysts, microelectronics, and batteries for their unique physical and chemical properties [1-3]. Usually, the cobalt oxide nanoparticles are prepared by using chemical or physical processes, including sol-gel method, chemical vapor deposition, and pulsed laser deposition, etc. [4-6]. In this work, we prepared the cobalt oxide nanoparticles by using the physical process of arc discharge, which was previously employed for the synthesis of metallic nanoparticles [7]. In the traditional arc discharge process, both the anode and the cathode are required to be highly electrically conductive. As a result, the arc discharge process is most suitable for the synthesis of metallic nanoparticles instead of the insulative oxide nanoparticles. However, the metallic nanoparticles generated by the arc discharge process may also transform into oxide nanoparticles with subsequent annealing in air [8]. In this work, we simplified the traditional arc discharge process and made it applicable for the direct one-step preparation of the oxide nanoparticles by using both conductive and insulative precursors.

The structure and magnetic properties of the cobalt oxide nanoparticles prepared by a variety of methods have been investigated extensively. Room-temperature ferromagnetism due to strained lattice configurations at the CoO/Co_3O_4 interface has been observed in antiferromagnetic cobalt oxide nanooctahedra prepared by thermal decomposition [9]. Weak ferromagnetism due to uncompensated surface magnetic moments has been reported in cobalt oxide nanoparticles prepared by wet chemical processing [10, 11]. In this work, the ferromagnetic behavior of the antiferromagnetic cobalt oxide nanoparticles prepared by a modified air plasma evaporation was studied. The exchange bias phenomenon was discovered by Meiklejohn and Bean in oxide-coated cobalt particles in 1956 [12]. Usually, the exchange bias phenomenon presents in interfaces between two kinds of substances with different magnetic orders, ferro/antiferromagnetic interface for instance. In this work, the exchange bias of the antiferromagnetic cobalt oxide nanoparticles with weak-ferromagnetic uncompensated surface spins was investigated.

2. Experimental

The commercial micro-powders of Co and Co_2O_3 were pressed into two thin cylinders, which were then fed to the high temperature region of the air plasma generated between a water-cooling copper anode and a tungsten

*Corresponding author: Tel: +86-571-86836063
e-mail: hongliang_ge@cjlu.edu.cn

cathode. The electrical current was maintained at 90 A for a period of time. The as-prepared nanoparticles were collected and analyzed by using a powder X-ray diffraction (XRD) with Cu $K\alpha$ radiation. The morphology of the samples was characterized with a Tecnai G2 F30 S-Twin transmission electron microscopy (TEM). The magnetic properties of the samples were measured by using a Quantum-Design magnetic properties measurement system in fields up to 7 T. The zero-field cooling (ZFC) and field (0.005 T) cooling (FC) *M-T* curves of the samples were measured by first cooling the samples from 400 to 14 K and then recording the magnetization of the samples under 0.005 T with increasing temperature.

3. Results and Discussion

The cobalt oxide nanoparticles prepared from Co and Co_2O_3 in air plasma are named as sample A and sample B, respectively. The XRD patterns for both Sample A and Sample B could be indexed with CoO and Co_3O_4, as shown in Fig. 1. For sample A, the relative intensity of CoO is stronger than that of Co_3O_4, indicating a larger fraction of CoO. However, the fraction of CoO is lower than that of Co_3O_4 for Sample B. The coexistence of CoO and Co_3O_4 in both samples was ascribed to the reactions as described by the following equilibrium: $2Co_3O_4 = 6CoO + O_2$. It is known that CoO converts to Co_3O_4 if heated to around 600-700 °C in air. Above 900 °C, CoO is stable. The results indicate that Co_2O_3 is not stable at high temperatures. The broadening of the XRD peaks were ascribed to the small crystalline size of the CoO and the Co_3O_4 phases. By using the Scherrer equation, the average crystalline size of CoO and Co_3O_4 in the samples

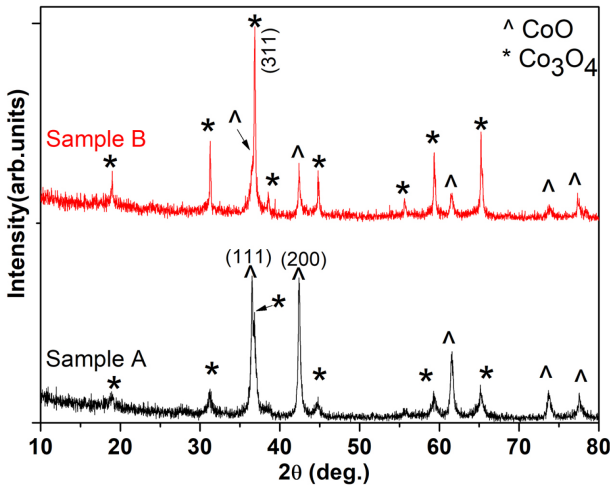

Fig. 1. (Color online) X-ray diffraction patterns of both Sample A and Sample B could be indexed with CoO and Co_3O_4.

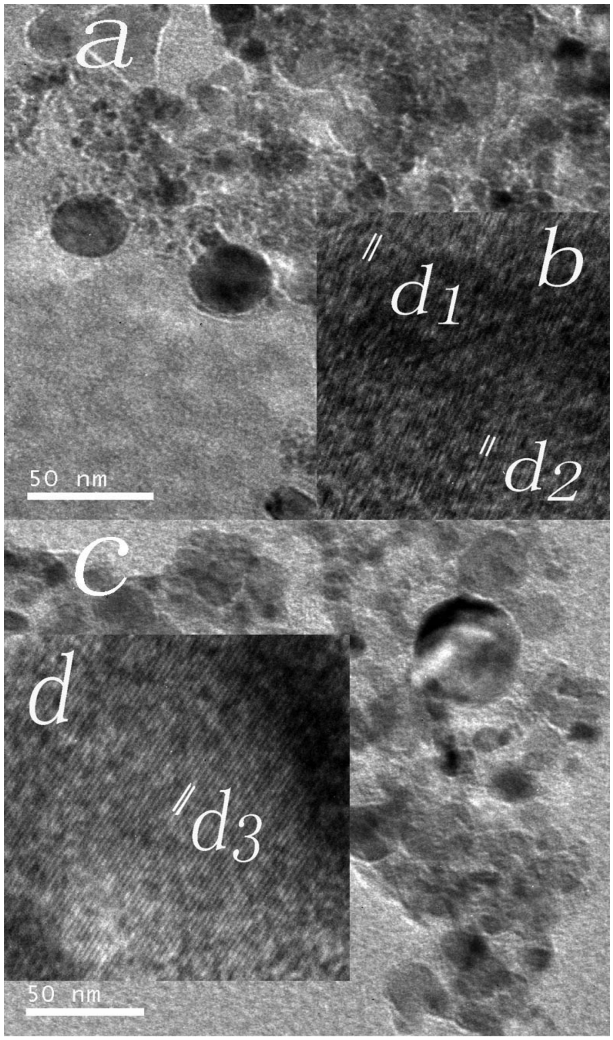

Fig. 2. (Color online) The TEM images of the nanoparticles prepared by air plasma evaporation of Co (a, b) and Co_2O_3 (c, d), respectively. The inter-planer spacing d_1= 0.2150 nm, d_2 = 0.2469 nm, and d_3 = 0.2429 nm.

was estimated to be ~25 nm and 35 nm, respectively.

Figure 2 shows the TEM images of the as-prepared nanoparticles. Most nanoparticles are spherical in shape with a relative narrow size distribution. The size of the nanoparticles in sample A is 10-30 nm, as shown in Fig. 2(a). The particle size observed by TEM agrees well with that estimated by XRD Scherrer equation as mentioned above. A high-resolution analysis on the surface layer of the as-prepared nano-powders is shown in Fig. 2(b), which shows an inter-planer spacing of $d_1 = 0.2150$ nm and $d_2 = 0.2496$ nm, corresponding to the (200) lattice spacing the (111) lattice spacing of CoO, respectively. However, a large number of defects and amorphous region could also be observed in Fig. 2(b). We ascribe the formation of the amorphous region to the rapid solidi-

fication of the atoms when leaving the high temperature region of the air plasma. Most nanoparticles in sample B are approximately 10-40 nm in size, as shown in Fig. 2(c). A high-resolution analysis on the surface layer of the as-prepared nano-powders is shown in Fig. 2(d), which shows an inter-planer spacing of $d_3 = 0.2429$ nm, corresponding to the (311) lattice spacing of Co_3O_4. The lattice spacings observed by TEM agrees well with the XRD results.

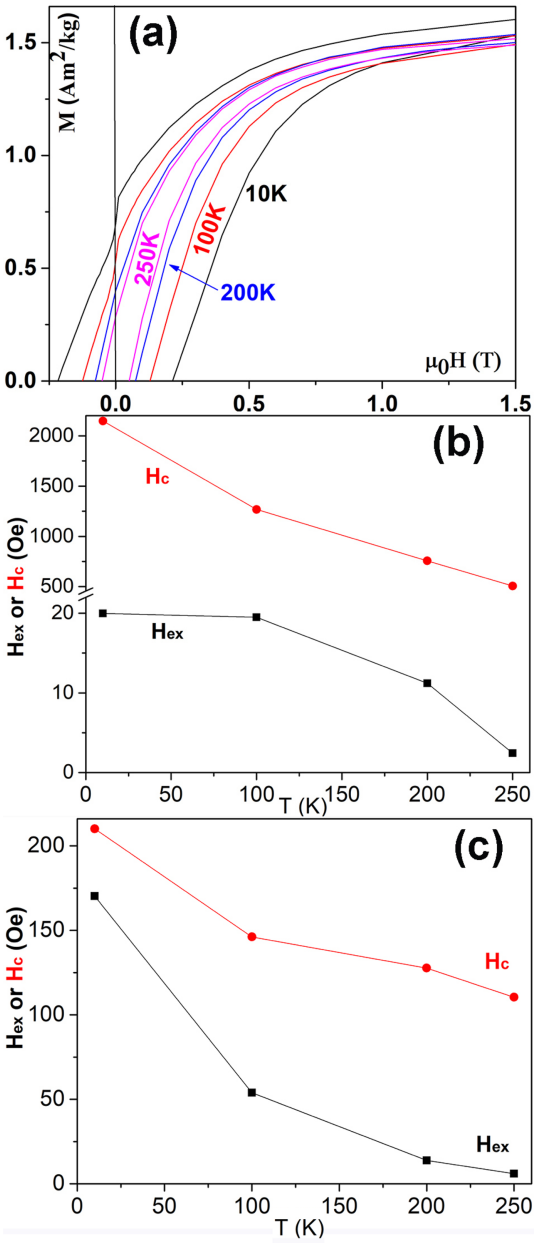

Fig. 3. (Color online) The M-H curves and the temperature dependence of coercivity and exchange bias in the as-prepared nanopowders: (a, b) for sample A, and (c) for sample B.

Figure 3 shows the magnetic properties of the as-prepared nano-powders at 10 K, 100 K, 200 K, and 250 K, respectively. Both sample A and sample B show obvious magnetic hysteresis and loop shifts, indicating the presence of ferromagnetic and antiferromagnetic regions in the samples. For sample A, the saturation magnetization M_s = 1.66 Am^2/kg at 10 K and M_s = 1.53 Am^2/kg at 250 K. The magnetization of sample B reaches 4.64 Am^2/kg at 10 K under 7 T, and 3.43 Am^2/kg at 250 K under 7 T. It should be noted that both CoO and Co_3O_4 are antiferromagnetic materials with a Néel temperature of 293 and 33 K, respectively. We ascribe the weak ferromagnetic behavior of the samples to the uncompensated surface spins and the disordered regions in the samples. The ferromagnetic mechanism originating from the uncompensated spins in the antiferromagnetic substances has been studied intensively. Ye et al, have reported greatly enhanced magnetization arising from the uncompensated surface spins in Co_3O_4 hollow nanospheres [11]. Zhang et al have reported antiferromagnetic Cr and Cr_2O_3 nanoparticles show weak ferromagnetic behaviors, owing to the uncompensated surface spins [13]. Lin *et al*. obtained the monodisperse MnO nanoparticles, which show a weak ferromagnetic behavior due to uncompensated surface spins at low temperatures [14].

An exchange bias due to the interfacial coupling between ferromagnetic uncompensated spins and the antiferromagnetic core was observed. The temperature dependences of the coercivity and the exchange bias of the samples are shown in Fig. 3(b, c). The coercivity of both sample A and sample B decreases with increasing temperature. An exchange bias up to 17.1 mT was observed in sample B.

The temperature dependence of magnetization of the cobalt oxide nanoparticles is shown in the Fig. 4. The magnetizations in the FC curves of both sample A and sample B decrease with increasing temperature, and this tendency has been observed in most ferromagnetic or antiferromagnetic nanoparticles [7, 13, 14]. It is interesting that the magnetization in the ZFC curves of both sample A and sample B increase with increasing temperature up to 350 K, and this tendency is very rare for most ferromagnetic or antiferromagnetic nanoparticles [7, 15]. The blocking temperatures of most antiferromagnetic or AFM/FM nanoparticles is lower than 350 K [14, 16]. However, the presence of ferro/antiferromagnetic exchange biased interface would beat the superparamagnetic limit of the ferromagnetic nanoparticles and result in an increase of the magnetization in ZFC curves [17], even though such behaviors in some samples are not so prominent [18]. The monotonic increase of magnetization in the ZFC curves at temperatures up to 350 K indicates a

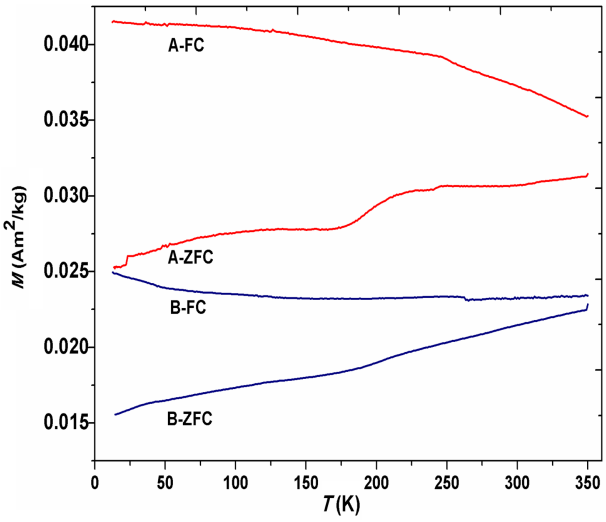

Fig. 4. (Color online) The ZFC and FC temperature dependence of magnetization of the as-prepared cobalt oxide nanoparticles of sample A and sample B, respectively.

higher blocking temperature. We ascribe the higher blocking temperature to the exchange bias effect, which provides an additional field to overcome thermal agitation of the magnetization reversal. Since the ferromagnetic region is in close contact with the AFM phase in our nanoparticles, it is possible for the ferromagnetic region being stabilized with exchange bias. It is known that a kind of ferrimagnetic behavior may be displayed in the antiferromagnetic phase when in an external magnetic field. The thermal contribution will cause disruption to the antiferromagnetic alignment of the AFM core and also result in an increase of magnetization with increasing temperature.

4. Conclusions

The cobalt oxide nano-particles were prepared by using a modified arc discharge process in air with conductive Co and insulative Co_2O_3 precursors, respectively. The cobalt oxides are spherical in shape with size ranging from 10 to 40 nm. Weak ferromagnetism and exchange bias in the cobalt oxide nanoparticles were studied. The uncompensated surface spins over the anti-ferromagnetic nanoparticles are the origin of the weak ferromagnetic behaviors.

Acknowledgements

We are grateful for the support from the National Natural Science Foundation of China (No. 51671177 and 11074227).

References

[1] F. Liu, H. Su, L. Jin, H. Zhang, X. Chu, and W. Yang, J. Colloid. Interface Sci. **505**, 796 (2017).
[2] F. Jiao and H. Frei, Angew. Chem. Int. Ed. **48**, 1841 (2009).
[3] K. Mizushima, P. C. Jones, P. J. Wiseman, and J. B. Goodenough, Mater. Res. Bull. **15**, 783 (1980).
[4] C. Lin, J. A. Ritter, and B. N. Popov, J. Electrochem. Soc. **145**, 4097 (1998).
[5] T. Maruyama and S. Arai, J. Electrochem. Soc. **143**, 1383 (1996).
[6] N. Patel, A. Santini, V. Bello, G. Mattei, and A. Miotello, Surf. Coat. Technol. **235**, 784 (2013).
[7] P. Z. Si, I. Skorvanek, J. Kovac, D. Y. Geng, X. G. Zhao, and Z. D. Zhang, J. Appl. Phys. **94**, 6779 (2003).
[8] P. Z. Si and Z. D. Zhang, Int. J. Mod. Phys. B **23**, 3895 (2009).
[9] N. Fontaina-Troitino, S. Liebana-Vinas, B. Rodriguez-Gonzalez, Z. A. Li, M. Spasova, M. Farle, and V. Salgueirino, Nano Lett. **14**, 640 (2014).
[10] A. Tomou, D. Gournis, I. Panagiotopoulos, Y. Huang, G. C. Hadjipanayis, and B. J. Kooi, J. Appl. Phys. **99**, 123915 (2006).
[11] Q. L. Ye, H. Yoshikawa, and K. Awaga, Materials **3**, 1244 (2010).
[12] W. P. Meiklejohn and C. P. Bean, Phys. Rev. **102**, 1413 (1956).
[13] W. S. Zhang, E. Bruck, Z. D. Zhang, O. Tegus, W. F. Li, P. Z. Si, D. Y. Geng, K. H. J. Buschow, Physica B **358**, 332 (2005).
[14] C. C. Lin, C. J. Chen, and R. K. Chiang, J. Cryst. Growth **338**, 152 (2012).
[15] H. G. Shi and X. M. He, J. Phys. Chem. Solids **73**, 646 (2012).
[16] H. T. Zhu, J. Luo, J. K. Liang, G. H. Rao, J. B. Li, J. Y. Zhang, and Z. M. Du, Physica B **403**, 3141 (2008).
[17] V. Skumrvey, S. Stoyanov, Y. Zhang, G. Hadjipanayis, D. Givord, and J. Nogues, Nature **423**, 850 (2003).
[18] D. L. Peng, K. Sumiyama, T. Hihara, S. Yamamuro, and T. J. Konno, Phys. Rev. B **61**, 3103 (2000).